

Fluctuation-induced free energy of thin peptide films

M. A. Baranov,¹ G. L. Klimchitskaya,^{2,1} V. M. Mostepanenko,^{2,1,3} and E. N. Velichko¹

¹*Institute of Physics, Nanotechnology and Telecommunications,
Peter the Great Saint Petersburg Polytechnic University, Saint Petersburg, 195251, Russia*

²*Central Astronomical Observatory at Pulkovo of the Russian
Academy of Sciences, Saint Petersburg, 196140, Russia*

³*Kazan Federal University, Kazan, 420008, Russia*

Abstract

We apply the Lifshitz theory of dispersion forces to find a contribution to the free energy of peptide films which is caused by the zero-point and thermal fluctuations of the electromagnetic field. For this purpose, using available information about the imaginary parts of dielectric permittivity of peptides, the analytic representation for permittivity of typical peptide along the imaginary frequency axis is devised. Numerical computations of the fluctuation-induced free energy are performed at room temperature for the freestanding peptide films, containing different fractions of water, and for similar films deposited on dielectric (SiO_2) and (Au) substrates. It is shown that the free energy of a freestanding peptide film is negative and, thus, contributes to its stability. The magnitude of the free energy increases with increasing fraction of water and decreases with increasing thickness of a film. For peptide films deposited on a dielectric substrate the free energy is nonmonotonous. It is negative for thicker than 100 nm films, reaches the maximum value at some film thickness, but vanishes and changes its sign for thinner than 100 nm films. The fluctuation-induced free energy of peptide films deposited on metallic substrate is found to be positive which makes films less stable. In all three cases, simple analytic expressions for the free energy of sufficiently thick films are found. The obtained results may be useful to attain film stability in the next generation of organic microdevices with further shrunk dimensions.

I. INTRODUCTION

In the last few years organic electronics has assumed great importance because of its value in many applications [1]. For thin protein and peptide films and coatings, it is possible to modulate their physical and functional properties as required in optical and electronic devices, biotechnology, and even in food packing [2–9]. In this connection, extensive studies of protein, peptide and other organic films have been performed (see, for instance, Refs. [10–17]).

It is well known that miniaturization is the main tendency in developing of modern electronic devices, and organic electronics is not an exception to this rule. A number of organic microdevices has already been created (see, e.g., Refs. [5, 18–20]). It was noticed that with decreasing thickness of an organic film to below a micrometer the problem of its stability acquires a serious meaning. There are several contributions to the free energy of a film which is responsible for its stability [21]. One of these contributions, which is gaining in importance with decreasing film thickness, is caused by the zero-point and thermal fluctuations of the electromagnetic field.

The fluctuation-induced force acting between two closely spaced material surfaces is the long-explored subject. At separations below a few nanometers it is of quantum but nonrelativistic character and is usually called the van der Waals force [22]. At larger separations the effects of relativistic retardation come into play and a frequently used name is the Casimir force [23]. The van der Waals and Casimir forces are also known under a generic name dispersion forces [24]. They can be calculated by using the Lifshitz theory [23, 25]. For organic films, including the protein ones, the dispersion forces have long been investigated by many authors (see, e.g., Refs. [26–29]).

The Lifshitz theory can be also used to calculate the fluctuation-induced free energy of a freestanding in vacuum or deposited on a material substrate thin film [21]. For this purpose, one should exploit the Lifshitz formula for a three-layer system and put equal to unity the dielectric permittivities of two or one outer layers, respectively. Investigations along these lines have been performed recently for metallic and dielectric films, both freestanding and deposited on substrates [30–35]. It was found that the fluctuation-induced free energy of a film can be both negative and positive, i.e., the effect of electromagnetic fluctuations may be both favorable and unfavorable to its stability. For organic films, however, the fluctuation-

induced contribution to the free energy was not investigated so far.

In this paper, we use the Lifshitz theory to calculate the free energy of a freestanding and deposited on a substrate peptide films. Both cases of dielectric (SiO_2) and metallic (Au) substrates are considered. The dielectric permittivity of a typical peptide is modeled over the wide range of imaginary frequencies by means of simple analytic representation. The free energy per unit area of peptide film is calculated at room temperature as a function of film thickness for different volume fractions of water contained in a film. It is shown that for a freestanding peptide film the fluctuation-induced free energy is negative. With increasing volume fraction of water in a film, the magnitude of the free energy increases by making the film more stable. For peptide films deposited on a SiO_2 substrate the free energy is negative for thicker than 100 nm films and its magnitude reaches the maximum value for the film of some definite thickness. For thinner than 100 nm film the free energy may vanish and even become positive with further decreased film thickness. It is shown that for protein films deposited on metallic substrates the fluctuation-induced free energy takes the positive values. The free energy again increases with increasing volume fraction of water, but this makes a film less stable. In all three cases, for films of more than $2 \mu\text{m}$ thickness, the fluctuation-induced free energy reaches the classical limit. In doing so, simple analytic representations for the fluctuation-induced free energy are obtained.

The paper is organized as follows. In Sec. II, main formulas for the fluctuation-induced free energy of both freestanding and deposited on a substrate composite films are represented. Section III contains modeling of the dielectric permittivity and calculations of the free energy for a freestanding peptide film. In Sec. IV, the fluctuation-induced free energies of peptide films deposited on dielectric and metallic substrates are found. Section V contains our conclusions and discussion.

II. GENERAL FORMALISM FOR FREESTANDING AND DEPOSITED ON A SUBSTRATE PEPTIDE FILMS

We consider the peptide film of thickness a described by the frequency-dependent dielectric permittivity $\varepsilon^{(f)}(\omega)$. Peptide and protein films are usually the composite layers. They are made up not of entirely peptide or protein but contain some volume fraction of a plasticizer to ensure the required physical and functional properties [3]. One of the plasti-

cizers discussed in the literature is water [36, 37] which is contained in organic films in any case. Because of this, below we consider the dielectric permittivity of peptide film, $\varepsilon^{(f)}$, as a combination of the dielectric permittivities of peptide in itself, $\varepsilon^{(p)}(\omega)$, and of water, $\varepsilon^{(w)}(\omega)$.

It is assumed that the peptide film is deposited on a dielectric or metallic substrate described by the dielectric permittivity $\varepsilon(\omega)$. The substrate is considered as a semispace when calculating the fluctuation-induced free energy of a film. For the validity of this approach, the dielectric substrate should be thicker than approximately 2 μm [38] and metallic substrate thicker than 100 nm [23]. If a peptide film is freestanding in vacuum, one should put $\varepsilon(\omega) = 1$ in all subsequent formulas. Assuming that the film is in thermal equilibrium with the environment at temperature T , the fluctuation-induced free energy of this film is given by the Lifshitz-type formula [23, 25, 33]

$$\mathcal{F}(a) = \frac{k_B T}{2\pi} \sum_{l=0}^{\infty} \int_0^{\infty} k dk \quad (1)$$

$$\times \sum_{\alpha} \ln \left[1 - r_{\alpha}^{(f,v)}(i\xi_l, k) r_{\alpha}^{(f,s)}(i\xi_l, k) e^{-2ak^{(f)}(i\xi_l, k)} \right].$$

Here, k_B is the Boltzmann constant, $r_{\alpha}^{(f,v)}$ and $r_{\alpha}^{(f,s)}$ are the reflection coefficients on the boundary surfaces between the peptide film and vacuum and substrate, respectively. These reflection coefficients are defined for two independent polarizations of the electromagnetic field, transverse magnetic ($\alpha = \text{TM}$) and transverse electric ($\alpha = \text{TE}$). They are calculated at the pure imaginary Matsubara frequencies $\xi_l = 2\pi k_B T l / \hbar$, $l = 0, 1, 2, \dots$, and k is the projection of the wave vector on the plane of a film. The prime on the first summation sign in Eq. (1) means that the term with $l = 0$ should be taken with the weight 1/2 and

$$k^{(f)}(i\xi_l, k) = \left[k^2 + \varepsilon^{(f)}(i\xi_l) \frac{\xi_l^2}{c^2} \right]^{1/2}. \quad (2)$$

The explicit expressions for the reflection coefficients are the following:

$$r_{\text{TM}}^{(f,v)}(i\xi_l, k) = \frac{k^{(f)}(i\xi_l, k) - \varepsilon^{(f)}(i\xi_l) k^{(v)}(i\xi_l, k)}{k^{(f)}(i\xi_l, k) + \varepsilon^{(f)}(i\xi_l) k^{(v)}(i\xi_l, k)},$$

$$r_{\text{TE}}^{(f,v)}(i\xi_l, k) = \frac{k^{(f)}(i\xi_l, k) - k^{(v)}(i\xi_l, k)}{k^{(f)}(i\xi_l, k) + k^{(v)}(i\xi_l, k)}, \quad (3)$$

and

$$r_{\text{TM}}^{(f,s)}(i\xi_l, k) = \frac{\varepsilon(i\xi_l) k^{(f)}(i\xi_l, k) - \varepsilon^{(f)}(i\xi_l) k^{(s)}(i\xi_l, k)}{\varepsilon(i\xi_l) k^{(f)}(i\xi_l, k) + \varepsilon^{(f)}(i\xi_l) k^{(s)}(i\xi_l, k)},$$

$$r_{\text{TE}}^{(f,s)}(i\xi_l, k) = \frac{k^{(f)}(i\xi_l, k) - k^{(s)}(i\xi_l, k)}{k^{(f)}(i\xi_l, k) + k^{(s)}(i\xi_l, k)}, \quad (4)$$

where

$$\begin{aligned} k^{(v)}(i\xi_l, k) &= \left(k^2 + \frac{\xi_l^2}{c^2} \right)^{1/2}, \\ k^{(s)}(i\xi_l, k) &= \left[k^2 + \varepsilon(i\xi_l) \frac{\xi_l^2}{c^2} \right]^{1/2}. \end{aligned} \quad (5)$$

Equations (2)–(5) depend on the dielectric permittivities of substrate, $\varepsilon(i\xi)$, and of peptide film, $\varepsilon^{(f)}(i\xi)$. A peptide film is the mixture of peptide itself with the dielectric permittivity $\varepsilon^{(p)}(i\xi)$, which consists of molecules of irregular shape, and of water with the dielectric permittivity $\varepsilon^{(w)}(i\xi)$ which, in our case, plays the role of a plasticizer. For the dielectric permittivities of water and peptide one can use the Clausius-Mossotti equation [39]

$$\frac{\varepsilon^{(w,p)}(i\xi) - 1}{\varepsilon^{(w,p)}(i\xi) + 2} = \frac{4\pi}{3} N^{(w,p)} \alpha^{(w,p)}(i\xi), \quad (6)$$

where $N^{(w,p)}$ and $\alpha^{(w,p)}$ are the numbers of molecules of water or peptide per unit volume and their polarizabilities, respectively. If Φ is the volume fraction of water in peptide film, then, assuming no volume change on mixing of randomly distributed peptide molecules with water, the permittivity of peptide film, $\varepsilon^{(f)}(i\xi)$, is obtained from the following mixing formula [40]:

$$\begin{aligned} \frac{\varepsilon^{(f)}(i\xi) - 1}{\varepsilon^{(f)}(i\xi) + 2} &= \frac{4\pi}{3} [\Phi N^{(w)} \alpha^{(w)}(i\xi) + (1 - \Phi) N^{(p)} \alpha^{(p)}(i\xi)] \\ &= \Phi \frac{\varepsilon^{(w)}(i\xi) - 1}{\varepsilon^{(w)}(i\xi) + 2} + (1 - \Phi) \frac{\varepsilon^{(p)}(i\xi) - 1}{\varepsilon^{(p)}(i\xi) + 2}. \end{aligned} \quad (7)$$

In the next two sections, Eqs. (1)–(5) and (7) are used to calculate the fluctuation-induced free energy of the freestanding and deposited on material substrates peptide films and to investigate its dependence on the film thickness and the fraction of water contained in the film.

III. DIELECTRIC PERMITTIVITY AND FREE ENERGY OF A FREESTANDING PEPTIDE FILM

We consider the freestanding peptide film of thickness a containing the volume fraction of water Φ . Thus, we put $\varepsilon(i\xi_l) = 1$ in Eqs. (1)–(5). To find the dielectric permittivity of a film, $\varepsilon^{(f)}(i\xi_l)$, one needs to know the dielectric permittivities of water, $\varepsilon^{(w)}(i\xi_l)$, and of peptide, $\varepsilon^{(p)}(i\xi_l)$.

There are several representations for the permittivity of distilled water in the literature [22, 40–42] which lead to approximately equal calculation results for the dispersion force. Below we use the representation of Ref. [42]

$$\varepsilon^{(w)}(i\xi_l) = 1 + \frac{B}{1 + \tau\xi_l} + \sum_{j=1}^{11} \frac{C_j}{1 + \left(\frac{\xi_l}{\omega_j}\right)^2 + \frac{g_j\xi_l}{\omega_j^2}}, \quad (8)$$

where $B = 76.8$ and $1/\tau = 1.08 \times 10^{11}$ rad/s are the parameters of the Debye term describing orientation of permanent dipoles. The oscillator terms in Eq. (8) with $j = 1, 2, \dots, 5$ correspond to infrared frequencies, whereas the terms with $j = 6, \dots, 11$ describe the contribution of ultraviolet frequencies. The values of the oscillator strengths C_j , oscillator frequencies ω_j and relaxation parameters g_j are presented in Table I. As a result, $\varepsilon^{(w)}(0) = 81.2$.

The dielectric properties of various proteins and peptides have been investigated by many authors (see e.g., Refs. [43–51]). The obtained results are, however, not sufficient for calculation of the free energy using the Lifshitz theory which requires detailed information on the dielectric permittivity over a wide frequency region from zero to far ultraviolet. Here we present simple analytic form for the dielectric permittivity of a peptide film using the numerical results of Refs. [52, 53] obtained for different peptides in the microwave and ultraviolet frequency regions, respectively.

For sufficiently thick films considered below the most important contribution to the fluctuation-induced free energy is given by the region from zero to microwave imaginary frequencies. Because of this, as the basic peptide sample for our calculation, we choose the electrically neutral 18-residue zinc finger peptide. The molecules of this peptide have size of a few nanometers and an irregular shape. As was shown in Ref. [52] by means of molecular-dynamics simulation, within the investigated frequency region up to microwave frequencies its dielectric properties are well described by the frequency-dependent complex dielectric permittivity.

The proposed representation for the dielectric permittivity of our peptide sample along the imaginary frequency axis is

$$\varepsilon^{(p)}(i\xi) = 1 + \varepsilon_D(i\xi) + \varepsilon_{\text{IR}}(i\xi) + \varepsilon_{\text{UV}}(i\xi), \quad (9)$$

where the second, third, and fourth terms on the right-hand side of Eq. (9) describe the contributions of microwave, infrared, and ultraviolet frequencies, respectively. Using the numerical results in Fig. 8 of Ref. [52], obtained for the imaginary part of dielectric permittivity

in the microwave region, and the Debye form for orientation polarization, we find

$$\varepsilon_D(i\xi) = \frac{C_D}{1 + \tau_D \xi}, \quad (10)$$

where $C_D = 9.47$ and $1/\tau = 2.46 \times 10^8$ rad/s. According to the results of Ref. [52], $\varepsilon^{(p)}(0) = 15$.

Unfortunately, information about the dielectric properties of zinc finger peptide in the infrared and ultraviolet frequency regions is not available. Within the ultraviolet frequency region, however, the imaginary part of the frequency-dependent dielectric permittivity of cyclic tripeptide RGD-4C was computed on the basis of first principles of quantum mechanics in Ref. [53]. Taking into account that the ultraviolet region makes rather small contribution to the free energy for considered film thicknesses and that a molecule of RGD-4C is rather similar to that of zinc finger peptide in both shape and size, one may expect that a replacement of ε_{UV} contribution to Eq. (9) with the one computed for RGD-4C will not lead to major errors.

The numerical results in Fig. 6 of Ref. [53] for the imaginary part of the permittivity of RGD-4C peptide in ultraviolet region lead to the following oscillator representation:

$$\varepsilon_{UV}(i\xi) = \sum_{i=1}^3 \frac{C_{UV}^{(i)}}{1 + \left(\frac{\xi}{\omega_{UV}^{(i)}}\right)^2 + \frac{g^{(i)}\xi}{(\omega_{UV}^{(i)})^2}}. \quad (11)$$

Here, the oscillator strengths $C_{UV}^{(i)} = 0.022, 0.020,$ and 0.191 , the oscillator frequencies $\omega_{UV}^{(i)} = 5.18, 6.10,$ and 12.5 eV, and the relaxation parameters $g^{(i)} = 0, 0,$ and 14.0 eV for $i = 1, 2,$ and 3 , respectively.

The contribution of infrared frequencies is modeled in the Ninham-Parsegian representation

$$\varepsilon_{IR}(i\xi) = \frac{C_{IR}}{1 + \frac{\xi^2}{\omega_{IR}^2}}, \quad (12)$$

where C_{IR} is determined from already known parameters

$$C_{IR} = \varepsilon^{(p)}(0) - C_D - \sum_{i=1}^3 C_{UV}^{(i)} = 4.3 \quad (13)$$

and typical value of the oscillator frequency is $\omega_{IR} = 6.28 \times 10^{13}$ rad/s [54].

In Fig. 1, the dielectric permittivities of peptide and water given by Eqs. (8) and (9)–(12), respectively, are shown as the functions of imaginary frequency normalized to the first

Matsubara frequency over the interval from $\xi = \xi_1$ to $\xi = 30\xi_1$. The top line in the same figure shows the dielectric permittivity of a silica glass which is discussed in Sec. IV as a substrate material. The values of all dielectric permittivities at zero frequency are indicated in the text.

The dielectric permittivities of peptide, $\varepsilon^{(p)}$, and of water, $\varepsilon^{(w)}$, have been combined by using the mixing formula in Eq. (7) to obtain the dielectric permittivity of peptide film. In Fig. 2 the permittivities of peptide film, $\varepsilon^{(f)}$, are shown as functions of the imaginary frequency normalized to the first Matsubara frequency by the four lines from bottom to top for the films containing 0, 0.1, 0.25, and 0.4 volume fractions of water. The respective static permittivities are equal to 15, 16.5, 19.2, and 22.9.

Now we are in a position to calculate the fluctuation-induced free energy of a freestanding peptide film. Computations were performed by Eqs. (1)–(7) at $T = 300$ K with $\varepsilon(i\xi_l) = 1$ (i.e., with no substrate) for all-peptide film and for a film containing 0.25 volume fraction of water (i.e., with the permittivities $\varepsilon^{(f)}$ shown by the bottom and second above the bottom lines in Fig. 2). The computational results for the magnitudes of the free energy as functions of film thickness are shown in Fig. 3 by the bottom and top lines for all-peptide film and for the film containing 0.25 fractions of water, respectively. In both cases the free energy for films of any thickness is negative which is favorable to film stability. In doing so, both the term with $l = 0$, $\mathcal{F}^{(l=0)}$, in Eq. (1) and the sum of all terms with $l \geq 1$, $\mathcal{F}^{(l \geq 1)}$, are negative (compare with the case of peptide films deposited on substrates considered in Sec. IV).

The magnitude of fluctuation-induced free energy decreases monotonously with increasing film thickness. An increase of the volume fraction of water in the film results in larger magnitude of the free energy for a film of the same thickness. As an example, for the all-peptide film of 100 nm thickness $|\mathcal{F}| = 8.938$ fJ/mm², but for the film of the same thickness with 25% of water one obtains $|\mathcal{F}| = 11.33$ fJ/mm². For the all-peptide and containing 25% of water films of 1 μ m thickness we find $|\mathcal{F}| = 0.07328$ and 0.07928 fJ/mm², respectively. For better visualization the case of thinner films from 100 to 300 nm thickness is shown on an inset to Fig. 3 where the free energy is plotted in an uniform scale.

Note that the above computations have been performed with omitted conductivity of peptide film at a constant current. The reason is that an inclusion of the dc conductivity of dielectric materials in calculation of the dispersion interaction leads to contradictions with the measurement data (see, e.g., Refs. [23, 55–57]). In our case of peptide films, however,

this inclusion has only a slight effect on the obtained values of the free energy.

For sufficiently thick peptide film one can obtain rather simple analytic expression for the free energy. In this case the dominant contribution to the free energy is given by the term of Eq. (1) with $l = 0$, whereas all terms with $l \geq 1$ are exponentially small. Preserving only the zero-frequency term in Eq. (1), one obtains

$$\mathcal{F}(a) = \frac{k_B T}{4\pi} \int_0^\infty k dk \ln \left[1 - r_{\text{TM}}^{(f,v)^2}(0) e^{-2ak} \right], \quad (14)$$

where, according to Eq. (3),

$$r_{\text{TM}}^{(f,v)}(0) = \frac{1 - \varepsilon^{(f)}(0)}{1 + \varepsilon^{(f)}(0)}. \quad (15)$$

Integrating in Eq. (14), we find the free energy of peptide film in the so-called classical limit

$$\mathcal{F}(a) = -\frac{k_B T}{16\pi a^2} \text{Li}_3 \left[r_{\text{TM}}^{(f,v)^2}(0) \right], \quad (16)$$

where $\text{Li}_n(z)$ is the polylogarithm function.

For the freestanding all-peptide films the approximate expression (16) gives more than 99% of the exact free energy for film thicknesses $a \geq 1.5 \mu\text{m}$. In this case $r_{\text{TM}}^{(f,v)}(0) = -0.875$ and

$$\text{Li}_3 \left[r_{\text{TM}}^{(f,v)^2}(0) \right] = 0.865. \quad (17)$$

For the peptide films containing 25% of water, we have $r_{\text{TM}}^{(f,v)}(0) = -0.901$ and

$$\text{Li}_3 \left[r_{\text{TM}}^{(f,v)^2}(0) \right] = 0.927. \quad (18)$$

In this case the approximate expression (16) contributes more than 99% of the exact free energy for films with more or equal to $1.6 \mu\text{m}$ thicknesses.

IV. FREE ENERGY OF PEPTIDE FILMS DEPOSITED ON DIELECTRIC AND METALLIC SUBSTRATES

We begin with the case of peptide film deposited on dielectric substrate made of silica glass SiO_2 . The dielectric permittivity of SiO_2 along the imaginary frequency axis, $\varepsilon(i\xi)$, was repeatedly used in calculations of the Casimir force [23]. An analytic representation for it in the Ninham-Parsegian representation is contained in Ref. [40] (see the top line in Fig. 1).

Computations of the fluctuation-induced free energy of peptide film deposited on SiO₂ substrate were done by Eqs. (1)–(5) at $T = 300$ K. The computational results for the magnitudes of the free energy of all-peptide film and films containing 0.1, 0.25, and 0.4 volume fractions of water as the functions of film thickness are shown in Fig. 4 by the four lines plotted from bottom to top, respectively. In these computations the dielectric permittivities of peptide films with different fractions of water shown by the four lines in Fig. 2 have been used.

In the region of film thickness from 100 nm to 2 μ m the free energy of peptide film remains negative. However, unlike the case of a freestanding film, here we have $\mathcal{F}^{(l=0)} < 0$ but $\mathcal{F}^{(l \geq 1)} > 0$. Because of this, the free energy is a nonmonotonous function of the film thickness. Intuitively, this behavior can be explained by the fact that the dielectric permittivity of SiO₂ is larger than the dielectric permittivities of both water and peptide at all nonzero Matsubara frequencies (see Fig. 1). The static dielectric permittivities of both water and peptide are, however, larger than of SiO₂. This relationship between the dielectric permittivities determines a nonmonotonous behavior of the free energy.

From Fig. 4 it is seen that the free energy reaches the maximum values equal to 0.835, 0.8739, 1.0674, and 1.4657 fJ/mm² for the films containing 0, 0.1, 0.25, and 0.4 volume fractions of water and having the thicknesses of 130, 135, 130, and 115 nm, respectively. For better visualization, the region of film thickness in the vicinities of maximum free energy is shown on an inset where the uniform energy scale is used. For the all-peptide film of 85 nm thickness the fluctuation-induced free energy vanishes, $\mathcal{F} = 0$, and for $a < 85$ nm one has $\mathcal{F} > 0$. Here we do not consider so thin films because this would demand a more exact expression for the dielectric permittivity of peptide at high frequencies for obtaining reliable computational results. The point is that in the ultraviolet frequency region the dielectric permittivity of the zinc finger peptide under consideration was approximated in Sec. III by that of the RGD peptide. As a result, for sufficiently thin films, where the contribution of ultraviolet frequencies becomes dominant, the computed values of the free energy of a film might be burdened by rather big error. Because of this it is also not reasonable to apply suggested expressions for determination of the Hamaker constant of peptide film, which corresponds to the nonrelativistic limit of the Lifshitz formula, i.e., to separation distances (film thicknesses) up to only a few nanometers [23].

The inset to Fig. 4 suggests that the dependence of the free energy of the fraction of

water Φ in a film deposited on a substrate may be more complicated than in the case of a freestanding film. To confirm this guess, in Fig. 5 we present the computational results for the free energy of peptide films with different thickness as the functions of Φ . The lines labeled 1, 2, 3, and 4 are plotted for the peptide films of 100, 130, 150, and 200 nm thickness deposited on a SiO₂ substrate. As is seen in Fig. 5, there is a peculiar interplay between the film thickness and the fraction of water in their combined effect on the free energy of peptide film deposited on a dielectric substrate.

As in the case of a freestanding film, for sufficiently thick peptide film deposited on a dielectric substrate one can present simple analytic expression for the free energy. It is given by the zero-frequency term of Eq. (1)

$$\mathcal{F}(a) = \frac{k_B T}{4\pi} \int_0^\infty k dk \ln \left[1 - r_{\text{TM}}^{(f,v)}(0) r_{\text{TM}}^{(f,s)}(0) e^{-2ak} \right], \quad (19)$$

where, according to Eq. (4),

$$r_{\text{TM}}^{(f,s)}(0) = \frac{\varepsilon(0) - \varepsilon^{(f)}(0)}{\varepsilon(0) + \varepsilon^{(f)}(0)} \quad (20)$$

and $r_{\text{TM}}^{(f,v)}(0)$ is given by Eq. (15).

Calculating the integral in Eq. (19), one obtains the free energy of peptide film in the classical limit

$$\mathcal{F}(a) = -\frac{k_B T}{16\pi a^2} \text{Li}_3 \left[r_{\text{TM}}^{(f,v)}(0) r_{\text{TM}}^{(f,s)}(0) \right]. \quad (21)$$

For deposited on a SiO₂ substrate peptide films with larger than 2.5 μm thickness, Eq. (21) contributes more than 99% of the free energy. For all-peptide films and for films containing 0.1, 0.25, and 0.4 volume fractions of water, one obtains

$$\text{Li}_3 \left[r_{\text{TM}}^{(f,v)}(0) r_{\text{TM}}^{(f,s)}(0) \right] = 0.562, 0.600, 0.660, \text{ and } 0.724, \quad (22)$$

respectively. This allows simple calculation of the fluctuation-induced free energy for sufficiently thick peptide films deposited on a SiO₂ substrate by using Eq. (21).

Now we consider peptide film deposited on a metallic substrate. As a substrate material, we choose Au which is often used in measurements of dispersion forces [23, 55]. So, starting from this point and below, $\varepsilon(i\xi)$ in Eqs. (1)–(5) means the dielectric permittivity of Au which is obtained from the measured optical data, extrapolated down to zero frequency using either the plasma or the Drude model, with the help of the Kramers-Kronig relation [23, 55]. In several experiments (see review in Refs. [23, 55, 58] and more modern measurements in

Refs. [59–62]) it was shown that the use of the Drude model extrapolation taking into account the relaxation properties of free electrons results in a dramatic contradiction with the measurement data, whereas the plasma model extrapolation brings the theory in perfect agreement with the data. Below we use the dielectric permittivity of Au obtained by means of the plasma model extrapolation. Note, however, that here the Drude-plasma choice leads to only minor differences between the obtained free energies of peptide film because the metallic layer serves as only a substrate.

Computations of the fluctuation-induced free energy have been performed by Eqs. (1)–(5) at $T = 300$ K for all-peptide film and for films containing 0.1, 0.25, and 0.4 volume fractions of water deposited on Au substrate. The computational results for all-peptide film and for a film containing 0.4 fraction of water as the functions of film thickness are shown in Fig. 6 by the bottom and top lines, respectively. As is seen in Fig. 6, in both cases the free energy of a film is positive. The radical difference from the case of a dielectric substrate is that here both contributions to the free energy, $\mathcal{F}^{(l=0)}$ and $\mathcal{F}^{(l \geq 1)}$, are positive. Because of this, the fluctuation-induced contribution to the free energy of peptide films deposited on metallic substrates makes them less stable.

The range of smaller film thicknesses is shown on the inset to Fig. 6 where the uniform energy scale is used. Here, the computational results for the free energy of all-peptide film and for films with 0.1, 0.25, and 0.4 fractions of water are shown as the functions of film thickness by the four lines plotted from bottom to top, respectively. From Fig. 6 it is seen that in the case of metallic substrate the free energy of peptide films increases monotonously with increasing volume fraction of water in the film. By way of example, for the all-peptide film of 100 nm thickness deposited on Au substrate we have $\mathcal{F} = 22.25$ fJ/mm², but for a similar film containing 25% of water $\mathcal{F} = 28.97$ fJ/mm². For 1 μ m thick all-peptide and containing 25% of water films one obtains $\mathcal{F} = 0.08116$ and 0.08539 fJ/mm², respectively. This is qualitatively similar to the case of a freestanding peptide film, but in the presence of metallic substrate the magnitudes of the fluctuation-induced free energy are larger.

We have also computed the free energy of a peptide film deposited on Au substrate as a function of the volume fraction of water Φ contained in the film. The computational results are shown in Fig. 7 as the functions of Φ by the bottom and top lines plotted for the films of 200 and 100 nm thickness. Here, as opposed to Fig. 5 plotted for a dielectric substrate, the free energy increases monotonously with Φ .

In the end of this section, we consider the case of sufficiently thick peptide films when the major contribution to the free energy (1) is given by the term with $l = 0$. In this case the free energy is again presented by Eq. (19) where $r_{\text{TM}}^{(f,v)}(0)$ is expressed by Eq. (15) and $r_{\text{TM}}^{(f,s)}(0) = 1$ in accordance to Eq. (20) because $\varepsilon(0) = \infty$. The integration in Eq. (19) results in

$$\mathcal{F}(a) = -\frac{k_B T}{16\pi a^2} \text{Li}_3 \left[r_{\text{TM}}^{(f,v)}(0) \right]. \quad (23)$$

For peptide films of more than $2.5 \mu\text{m}$ thickness deposited on Au substrate Eq. (23) gives approximately 99% of the fluctuation-induced free energy. Thus, for sufficiently thick all-peptide and containing 0.1, 0.25, and 0.4 volume fractions of water films deposited on Au substrate we have

$$\text{Li}_3 \left[r_{\text{TM}}^{(f,v)}(0) \right] = -0.798, -0.806, -0.820, \text{ and } -0.832, \quad (24)$$

respectively, and one can calculate the fluctuation-induced free energy using Eq. (23).

V. CONCLUSIONS AN DISCUSSIONS

In this paper, we have considered the contribution to the free energy of peptide films which is induced by the zero-point and thermal fluctuations of the electromagnetic field. This contribution may become relatively large for sufficiently thin films and should be taken into account in the balance of energies responsible for the stability of a film. Taking into account that thin peptide, protein and other organic films are already used as constituent parts of various microdevices discussed in Sec. I, the role of quantum fluctuations in such films deserves attention.

The formalism allowing calculation of the fluctuation-induced free energy of peptide films, both freestanding and deposited on a substrate, is based on the Lifshitz theory of dispersion forces. Application of this formalism requires knowledge of the dielectric permittivities of all involved materials over the wide ranges of imaginary frequencies. Using the available numerical data for the imaginary parts of dielectric permittivities of peptides, we have devised an analytic expression for the dielectric permittivity of a typical peptide along the imaginary frequency axis. This permittivity was combined with the dielectric permittivity of different volume fractions of water to obtain the dielectric permittivity of a peptide film.

The numerical computations of the fluctuation-induced free energy have been performed at room temperature for a freestanding peptide film and for films deposited on dielectric (SiO_2) and metallic (Au) substrates. It is shown that the free energy of a freestanding film is always negative and, thus, contributes to the film stability. The magnitude of the free energy decreases with increasing film thickness, but increases with increasing fraction of water contained in the film.

For peptide films deposited on a SiO_2 substrate, the fluctuation-induced free energy is shown to be a nonmonotonous function of the film thickness. With increasing thickness of a film, the magnitude of the free energy reaches its maximum value (for thicknesses in the region from 115 to 135 nm depending on the fraction of water) and then decreases. For thinner than 100 nm films deposited on a SiO_2 substrate the fluctuation-induced free energy may vanish (for 85 nm thick all-peptide film) and even become positive. The dependence of the free energy on the fraction of water in the film deposited on a SiO_2 substrate demonstrates a nontrivial character dictated by the film thickness. Intuitively, this can be explained by the fact that with increasing fraction of water the dielectric permittivity of a film increases at all Matsubara frequencies. At zero Matsubara frequency this increase is, however, relatively larger than at nonzero Matsubara frequencies. For different film thicknesses the relative contribution of zero and nonzero Matsubara frequencies to the free energy varies resulting in a nontrivial dependence on the fraction of water.

The case of peptide films deposited on metallic (Au) substrate possesses important special features. According to our results, the fluctuation-induced free energy of peptide films in this case is always positive and, thus, makes the film less stable. The free energy decreases monotonously with increasing film thickness and increases with increasing fraction of water in the film.

To understand the role of fluctuation-induced phenomena in stability of peptide films, it would be interesting to compare the computed free energy with cohesive energies that are responsible for stability of these films. Taking into account a lack of information for specific films under consideration, it is possible to make only a qualitative estimation. Thus, for the mussel-inspired peptide films of 3–5 nm thickness deposited on substrates made of different materials the cohesive energy was measured to be of order 1 mJ/m^2 [63–66]. This value is contributed by the ionic or electrostatic interactions, hydrogen bonding, hydrophilic forces, fluctuation phenomena etc. To make a comparison, we scale, e.g., the fluctuation-induced

free energy of our peptide film of 100 nm thickness with 10% fraction of water deposited on Au substrate ($\mathcal{F} = 25.08 \text{ nJ/m}^2$) to 3–5 nm thickness using the scaling law $\sim a^{2.56}$ and obtain \mathcal{F} varying from 0.2 to 0.05 mJ/m², respectively. Thus, the fluctuation-induced free energy may contribute from 5 to 20% of the cohesive energy of a film.

For sufficiently thick peptide films, simple analytic expressions for their fluctuation-induced free energy are obtained. These expressions give 99% of the free energy for thicker than 1.5–1.6 μm freestanding films and for thicker than 2.5 μm films deposited on dielectric or metallic substrates.

In the future, it would be interesting to assess an applicability of the obtained results to different kinds of peptide and, even wider, protein and organic films of various constitutions. This might be helpful for resolving the problem of film stability when developing the next generation of organic microdevices with further shrunk dimensions.

Acknowledgments

The work of V. M. M. was partially supported by the Russian Government Program of Competitive Growth of Kazan Federal University.

-
- [1] G. Meller and T. Grasser (eds.), *Organic Electronics* (Springer, Heidelberg, 2010).
 - [2] C. D. Dimitrakopoulos and P. R. L. Malenfant, Organic Thin Film Transistors for Large Area Electronics, *Advanced Materials* **14**, 99 (2002).
 - [3] A. Gennadios (ed.), *Protein-Based Films and Coatings* (CRC Press, Boca Raton, 2002).
 - [4] Bin Zheng, D. T. Haynie, Hua Zhong, K. Sabnis, V. Surpuriya, N. Pargaonkar, G. Sharma, and K. Vistakula, Design of peptides for thin films, coatings and microcapsules for applications in biotechnology, *J. Biomater. Sci., Polymer Edit.* **16**, 285 (2005).
 - [5] R. Y. Yada (ed.), *Proteins in Food Processing* (Woodhead Publishing, Duxford, 2018).
 - [6] M. Natesan and R. G. Ulrich, Protein microarrays, and biomarkers of infection disease, *Int. J. Mol. Sci.* **11**, 5165 (2010).
 - [7] E. N. Velichko, M. A. Baranov, E. K. Nepomnyashchaya, A. V. Cheremiskina, and E. T. Aksenov, Studies of biomolecular nanomaterials for application in electronics and communi-

- cations. In: S. Balandin, S. Andreev, and Y. Kouchryavy (eds.), *Internet of Things, Smart Spaces, and Next Generation Networks and Systems* (Springer, Cham, 2015).
- [8] Chun-Yi Lee, Jenn-Chang Hwang, Yu-Lun Chueh, Ting-Hao Chang, Yi-Yun Cheng, Ping-Chiang Lyu, Hydrated bovine serum albumin as the gate dielectric material for organic field-effect transistors, *Org. Electr.* **14**, 2645 (2013).
- [9] Mingchao Ma, Xinjun Xu, Leilei Shi, and Lidong Li, Organic field-effect transistors with a low driving voltage using albumin as the dielectric layer, *RSC Advances* **4**, 58720 (2014).
- [10] A. Nayak and K. A. Suresh, Conductivity of Langmuir-Blodgett films of a disk-shaped liquid-crystalline molecule-DNA complex studied by current-sensing atomic force microscopy, *Phys. Rev. E* **78**, 021606 (2016).
- [11] A. Ulman, *An Introduction to Ultrathin Organic Films: From Langmuir-Blodgett to Self-Assembly* (Academic Press Limited, London, 1991).
- [12] A. Fang and M. Haataja, Crystallization in organic semiconductor thin films: A diffuse-interface approach, *Phys. Rev. E* **89**, 022407 (2014).
- [13] Jinmao Yan, Yunxiang Pan, A. G. Cheetham, Yi-An Lin, Wei Wang, Honggang Cui, and Chang-Jun Liu, One-Step Fabrication of Self-Assembled Peptide Thin Films with Highly Dispersed Noble Metal Nanoparticles, *Langmuir* **29**, 16051 (2013).
- [14] B. Li, D. T. Haynie, N. Palath, and D. Janisch, Nanoscale biomimetics: fabrication and optimization of stability of peptide-based thin films, *J. Nanosci. Nanotech.* **5**, 2042 (2005).
- [15] J. Ryu and C. B. Park, Solid-Phase Growth of Nanostructures from Amorphous Peptide Thin Films: Effect of Water Activity and Temperature, *Chem. Mater.* **20**, 4284 (2008).
- [16] M. A. Baranov, E. N. Velichko, and E. T. Aksenov, Method of nondestructive testing in the study of self-organization processes in the protein films, *J. Phys.: Conf. Ser.* **917**, 062059 (2017).
- [17] A. Laschitsch, B. Menges, and D. Johannsmann, Simultaneous determination of optical and acoustic thicknesses of protein layers using surface plasmon resonance spectroscopy and quartz crystal microweighing, *Appl. Phys. Lett.* **77**, 2252 (2000).
- [18] S. Sharma, R. W. Johnson, and T. A. Desai, Evaluation of the stability of nonfouling ultrathin poly(ethylene glycol) films for silicon-based microdevices, *Langmuir* **20**, 348 (2004).
- [19] H. Chandra, P. J. Reddy, and S. Srivastava, Protein microarrays and novel detection platforms, *Expert Rev. Proteomics* **8**, 61 (2011).

- [20] C.-K. Chou, N. Jing, H. Yamaguchi, P.-H. Tsou, H.-H. Lee, C.-T. Chen, Y.-N. Wang, S. Hong, C. Su, J. Kameoka, and M.-C. Hung, Rapid detection of two-protein interaction with a single fluorophore by using a microfluidic device, *Analyst* **135**, 2907 (2010).
- [21] I. Boinovich and A. Emelyanenko, Wetting and surface forces, *Adv. Coll. Interface Sci.* **165**, 60 (2011).
- [22] V. A. Parsegian, *Van der Waals Forces: A Handbook for Biologists, Chemists, Engineers, and Physicists* (Cambridge University Press, Cambridge, 2005).
- [23] M. Bordag, G. L. Klimchitskaya, U. Mohideen, and V. M. Mostepanenko, *Advances in the Casimir Effect* (Oxford University Press, Oxford, 2015).
- [24] J. Mahanty and B. W. Ninham, *Dispersion Forces* (Academic Press, London, 1976).
- [25] E. M. Lifshitz and L. P. Pitaevskii, *Statistical Physics, Pt. II* (Pergamon Press, Oxford, 1980).
- [26] V. A. Parsegian and B. W. Ninham, Application of the Lifshitz theory to the calculation of van der Waals forces across thin lipid films, *Nature* **224**, 1197 (1972).
- [27] S. Nir, Van der Waals interactions between surfaces of biological interest, *Progr. Surf. Sci.* **8**, 1 (1976).
- [28] C. M. Roth, B. L. Neal, and A. M. Lenhoff, Van der Waals interactions involving proteins, *Biophys. J.* **70**, 977 (1996).
- [29] Bing-Sui Lu and R. Podgornik, Effective interactions between fluid membranes, *Phys. Rev. E* **92**, 022112 (2015).
- [30] G. L. Klimchitskaya and V. M. Mostepanenko, Casimir free energy of metallic films: Discriminating between Drude and plasma model approaches, *Phys. Rev. A* **92**, 042109 (2015).
- [31] G. L. Klimchitskaya and V. M. Mostepanenko, Casimir and van der Waals energy of anisotropic atomically thin metallic films, *Phys. Rev. B* **92**, 205410 (2015).
- [32] G. L. Klimchitskaya and V. M. Mostepanenko, Casimir free energy and pressure for magnetic metal films, *Phys. Rev. B* **94**, 045404 (2016).
- [33] G. L. Klimchitskaya and V. M. Mostepanenko, Characteristic properties of the Casimir free energy for metal films deposited on metallic plates, *Phys. Rev. A* **93**, 042508 (2016).
- [34] G. L. Klimchitskaya and V. M. Mostepanenko, Low-temperature behavior of the Casimir free energy and entropy of metallic films, *Phys. Rev. A* **95**, 012130 (2017).
- [35] G. L. Klimchitskaya and V. M. Mostepanenko, Casimir free energy of dielectric films: Classical limit, low-temperature behavior and control, *J. Phys.: Condens. Matter* **29**, 275701 (2017).

- [36] N. Gontard and S. Ring, Edible wheat gluten film: Influence of water content on glass transition temperature, *J. Agric. Food Chem.* **44**, 3474 (1996).
- [37] J. M. Krochta, Proteins as Raw Materials for Films and Coatings: Definitions, Current Status, and Opportunities. In: A. Gennadios (ed.), *Protein-Based Films and Coatings* (CRC Press, Boca Raton, 2002), p. 1.
- [38] G. L. Klimchitskaya and V. M. Mostepanenko, Observability of thermal effects in the Casimir interaction with graphene-coated substrates, *Phys. Rev. A* **89**, 052512 (2014).
- [39] J. D. Jackson, *Classical Electrodynamics* (Wiley, New York, 1999).
- [40] D. B. Hough and L. H. White, The calculation of Hamaker constant from Lifshitz theory with application to wetting phenomena, *Adv. Coll. Interface Sci.* **14**, 3 (1980).
- [41] V. A. Parsegian and G. H. Weiss, Spectroscopic parameters for computation of van der Waals forces, *J. Coll. Interface Sci.* **81**, 285 (1981).
- [42] L. Bergström, Hamaker constant of inorganic materials, *Adv. Coll. Interface Sci.* **70**, 125 (1997).
- [43] T. L. McMeekin, M. L. Groves, and N. J. Hipp, Refractive indices of amino acids, proteins, and related substances, *Adv. Chem.* **44**, 54 (1964).
- [44] T. Inagaki, R. N. Hamm, E. T. Arakawa, and R. D. Birkhoff, Optical properties of bovine plasma albumin between 2 and 82 eV, *Biopolymers* **14**, 839 (1975).
- [45] H. Arwin, Optical properties of thin layers of bovine serum albumin, γ -globulin, and hemoglobin, *Appl. Spectrosc.* **40**, 313, (1986).
- [46] J. W. Pitera, M. Falta, and W. F. van Gunstern, Dielectric Properties of Proteins from Simulation: The Effect of Solvent, Ligands, pH, and Temperature, *Biophys. J.* **80**, 2546 (2001).
- [47] S. D. Figueiro, J. C. Goes, R. A. Moreira, and A. S. B. Sombra, On the physico-chemical and dielectric properties of glutaraldehyde crosslinked galactomannan-collagen films, *Carbohydrate Polymers* **56**, 313 (2004).
- [48] M. S. Venkatesh and G. S. V. Raghavan, An overview of microwave processing and dielectric properties of agri-food materials, *Biosyst. Eng.* **88**, 1 (2004).
- [49] M. Rabe, D. Verdes, and S. Seeger, Understanding protein adsorption phenomena at solid surfaces, *Adv. Coll. Interface Sci.* **162**, 87 (2011).
- [50] L. Li, C. Li, Z. Zhang, and E. Alexov, On the dielectric “constant” of proteins: smooth di-

- electric function for macromolecular modelling and its implementation in DelPhi, *J. Chem. Theory Comput.* **9**, 2126 (2013).
- [51] T. A. T. Sousa, L. C. Oliveira, F. H. Neff, H. M. Laborde, and A. M. N. Lima, Numerical tool for estimating the dielectric constant, the thickness, and the coverage of immobilized inhomogeneous protein films on gold in aqueous solution, *Appl. Opt.* **57**, 6866 (2018).
- [52] G. Löffler, H. Schreiber, and O. Steinhauser, Calculation of the Dielectric Properties of a Protein and its Solvent: Theory and a Case Study, *J. Mol. Biol.* **270**, 520 (1997).
- [53] P. Adhikari, A. M. Wen, R. H. French, V. A. Parsegian, N. F. Steinmetz, R. Podgornik, and W.-Y. Ching, Electronic Structure, Dielectric Response, and Surface Charge Distribution of RGD (1FUUV) Peptide, *Scient. Rep.* **4**, 5605 (2014).
- [54] F. Bibi, M. Villain, C. Guillaume, B. Sorli, and N. Gontard, A Review: Origin of Dielectric Properties of Proteins and Potential Development of Bio-Sensors, *Sensors* **16**, 1232 (2016).
- [55] G. L. Klimchitskaya, U. Mohideen, and V. M. Mostepanenko, The Casimir force between real materials: Experiment and theory, *Rev. Mod. Phys.* **81**, 1827 (2009).
- [56] C.-C. Chang, A. A. Banishev, G. L. Klimchitskaya, V. M. Mostepanenko, and U. Mohideen, Reduction of the Casimir Force from Indium Tin Oxide Film by UV Treatment, *Phys. Rev. Lett.* **107**, 090403 (2011).
- [57] A. A. Banishev, C.-C. Chang, R. Castillo-Garza, G. L. Klimchitskaya, V. M. Mostepanenko, and U. Mohideen, Modifying the Casimir force between indium tin oxide plate and Au sphere, *Phys. Rev. B* **85**, 045436 (2012).
- [58] V. B. Bezerra, R. S. Decca, E. Fischbach, B. Geyer, G. L. Klimchitskaya, D. E. Krause, D. López, V. M. Mostepanenko, and C. Romero, Comment on “Temperature dependence of the Casimir effect,” *Phys. Rev. E* **73**, 028101 (2006).
- [59] A. A. Banishev, C.-C. Chang, G. L. Klimchitskaya, V. M. Mostepanenko, and U. Mohideen, Measurement of the gradient of the Casimir force between a nonmagnetic gold sphere and a magnetic nickel plate, *Phys. Rev. B* **85**, 195422 (2012).
- [60] A. A. Banishev, G. L. Klimchitskaya, V. M. Mostepanenko, and U. Mohideen, Demonstration of the Casimir Force Between Ferromagnetic Surfaces of a Ni-Coated Sphere and a Ni-Coated Plate, *Phys. Rev. Lett.* **110**, 137401 (2013).
- [61] A. A. Banishev, G. L. Klimchitskaya, V. M. Mostepanenko, and U. Mohideen, Casimir interaction between two magnetic metals in comparison with nonmagnetic test bodies, *Phys. Rev. B*

- 88**, 155410 (2013).
- [62] G. Bimonte, D. López, and R. S. Decca, Isoelectronic determination of the thermal Casimir force, *Phys. Rev. B* **93**, 184434 (2016).
- [63] T. H. Anderson, J. Yu, A. Estrada, M. U. Hammer, J. H. Waite, and J. N. Israelachvili, The Contribution of DOPA to SubstratePeptide Adhesion and Internal Cohesion of Mussel-Inspired Synthetic Peptide Films, *Adv. Funct. Mater.* **20**, 4196 (2010).
- [64] Q. Lu, E. Danner, J. H. Waite, J. N. Israelachvili, H. Zeng, and D. S. Hwang, Adhesion of mussel foot proteins to different substrate surfaces, *J. R. Soc. Interface* **10**, 20120759 (2013).
- [65] S. Das, N. R. Martinez Rodriguez, W. Wei, J. H. Waite, and J. N. Israelachvili, Peptide Length and Dopa Determine Iron-Mediated Cohesion of Mussel Foot Proteins, *Adv. Funct. Mater.* **25**, 5840 (2015).
- [66] Z. A. Levine, M. V. Rapp, W. Wei, R. G. Mullen, C. Wu, G. H. Zerze, J. Mittal, J. H. Waite, J. N. Israelachvili, and J.-E. Shea, Surface force measurements and simulations of mussel-derived peptide adhesives on wet organic surfaces, *PNAS* **113**, 4332 (2016).

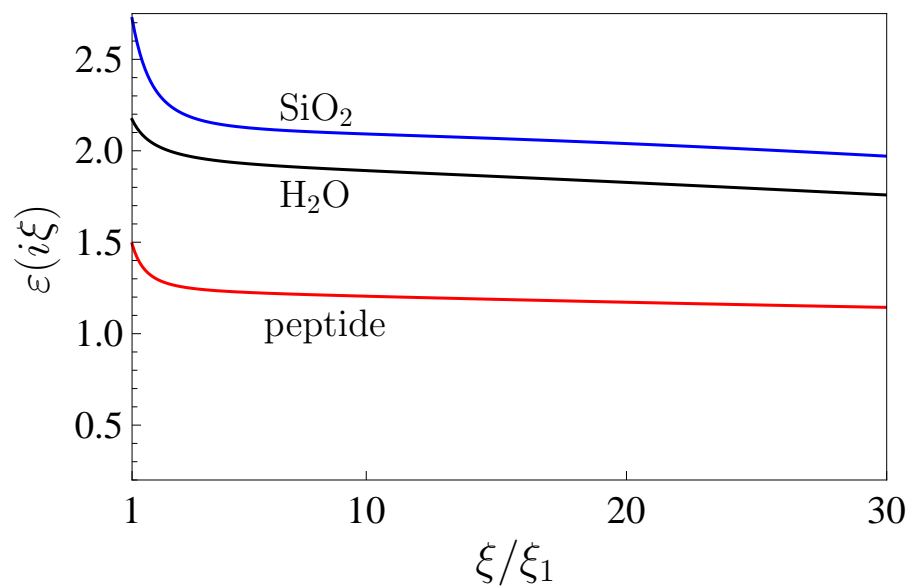


FIG. 1: The dielectric permittivities of peptide, water and silica glass are shown as the functions of imaginary frequency normalized to the first Matsubara frequency by the three lines plotted from bottom to top, respectively.

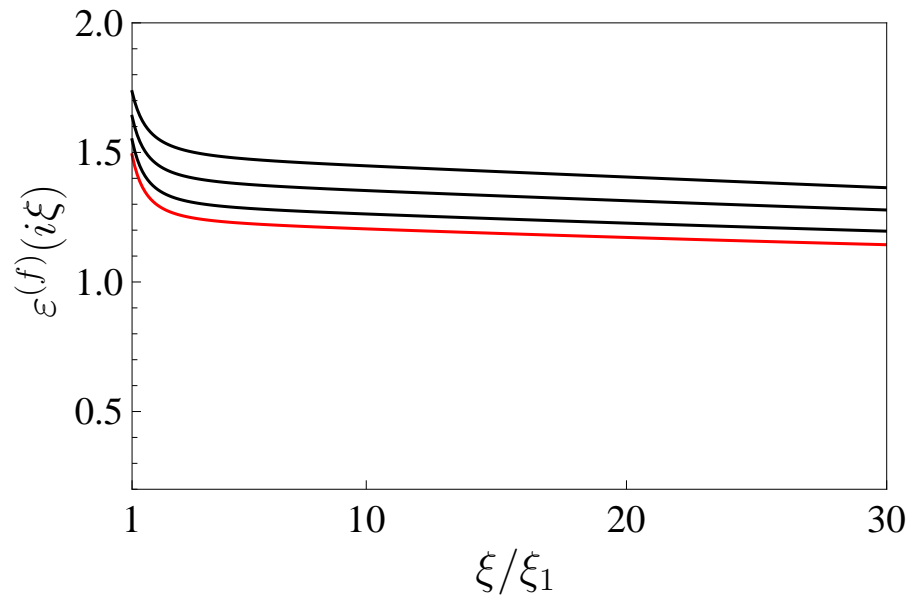


FIG. 2: The dielectric permittivities of peptide films containing 0, 0.1, 0.25, and 0.4 volume fractions of water are shown as the functions of imaginary frequency normalized to the first Matsubara frequency by the four lines plotted from bottom to top, respectively.

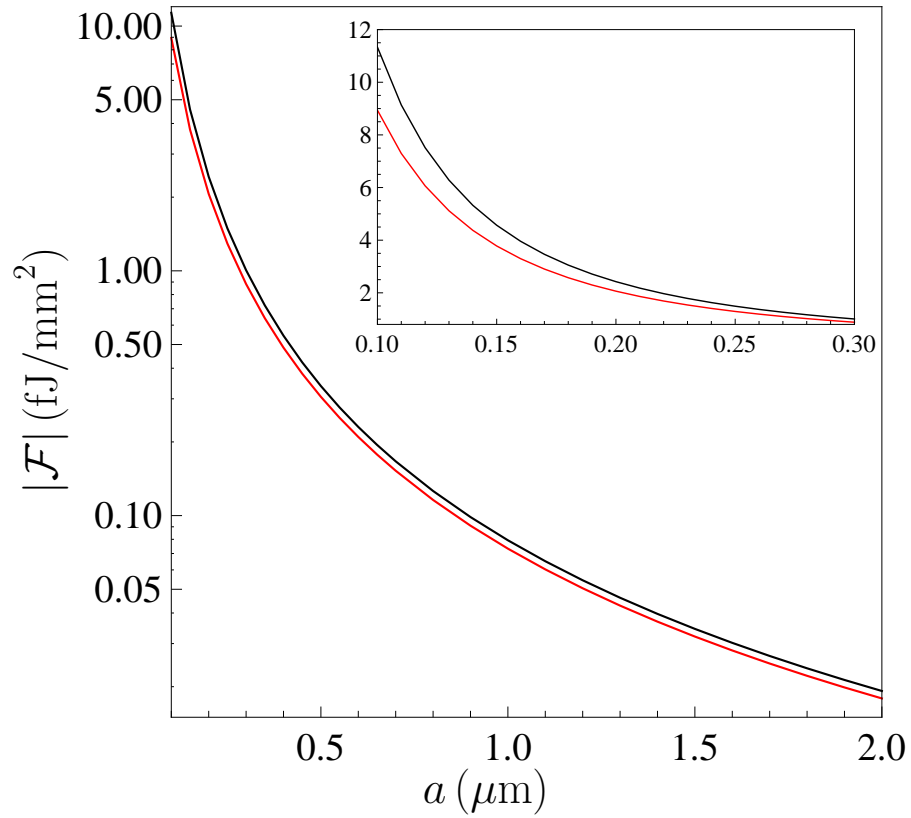


FIG. 3: The magnitudes of the fluctuation-induced free energies of peptide films containing 0 and 0.25 volume fractions of water are shown as the functions of film thickness by the two lines plotted from bottom to top, respectively. In an inset, the case of thinner films is illustrated using an uniform energy scale.

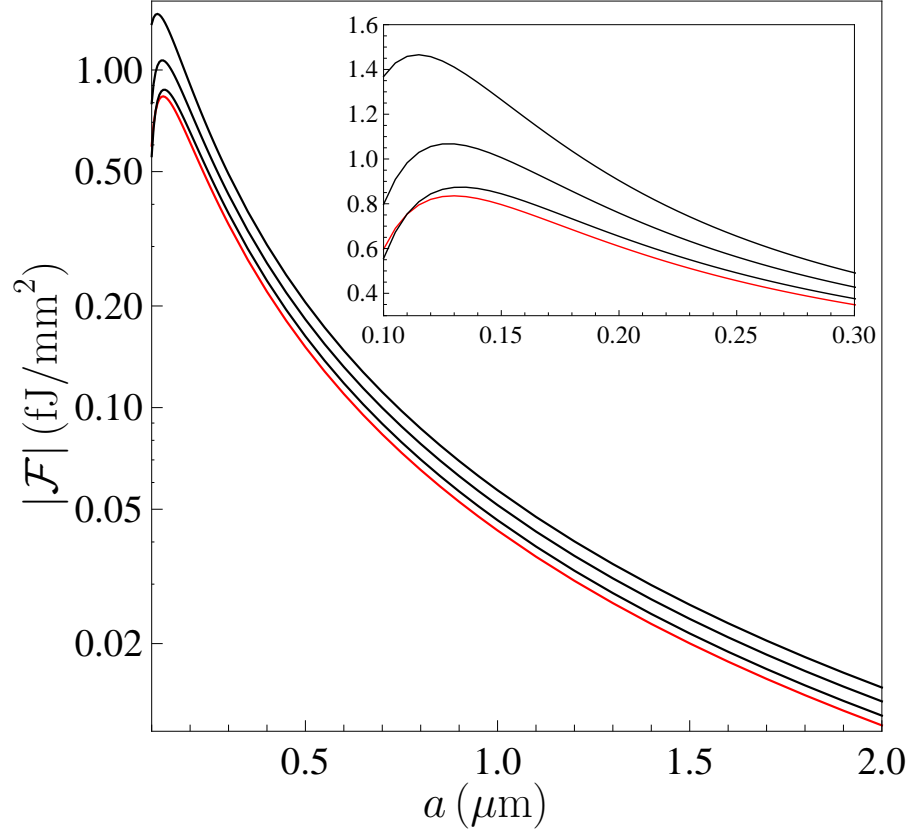


FIG. 4: The magnitudes of the fluctuation-induced free energies of peptide films, deposited on SiO_2 substrate, which contain 0, 0.1, 0.25, and 0.4 volume fractions of water, are shown as the functions of film thickness by the four lines plotted from bottom to top, respectively. In an inset, the case of thinner films is illustrated using an uniform energy scale.

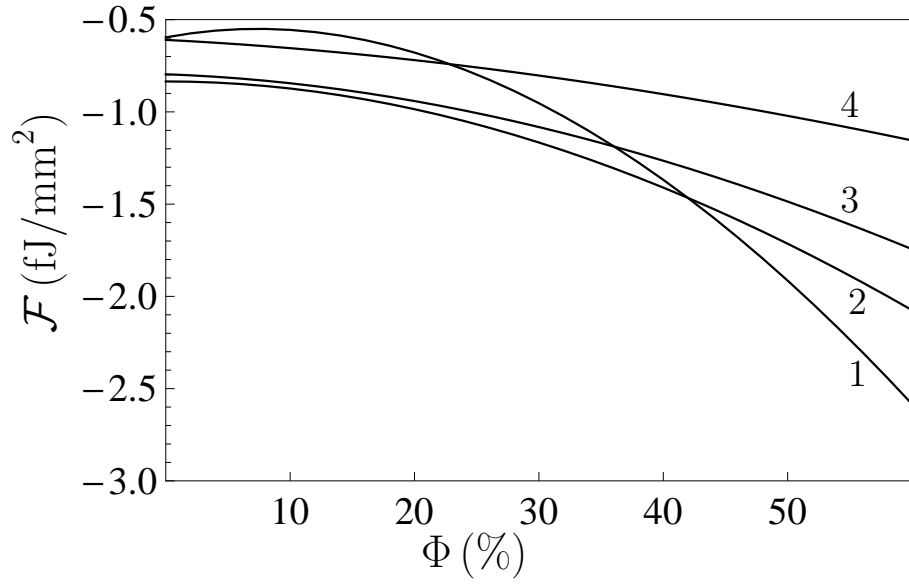


FIG. 5: The fluctuation-induced free energies of peptide films of thicknesses 100, 130, 150, and 200 nm deposited on a SiO_2 substrate are shown as the functions of the fractions of water in the film by the four lines labeled 1, 2, 3, and 4, respectively.

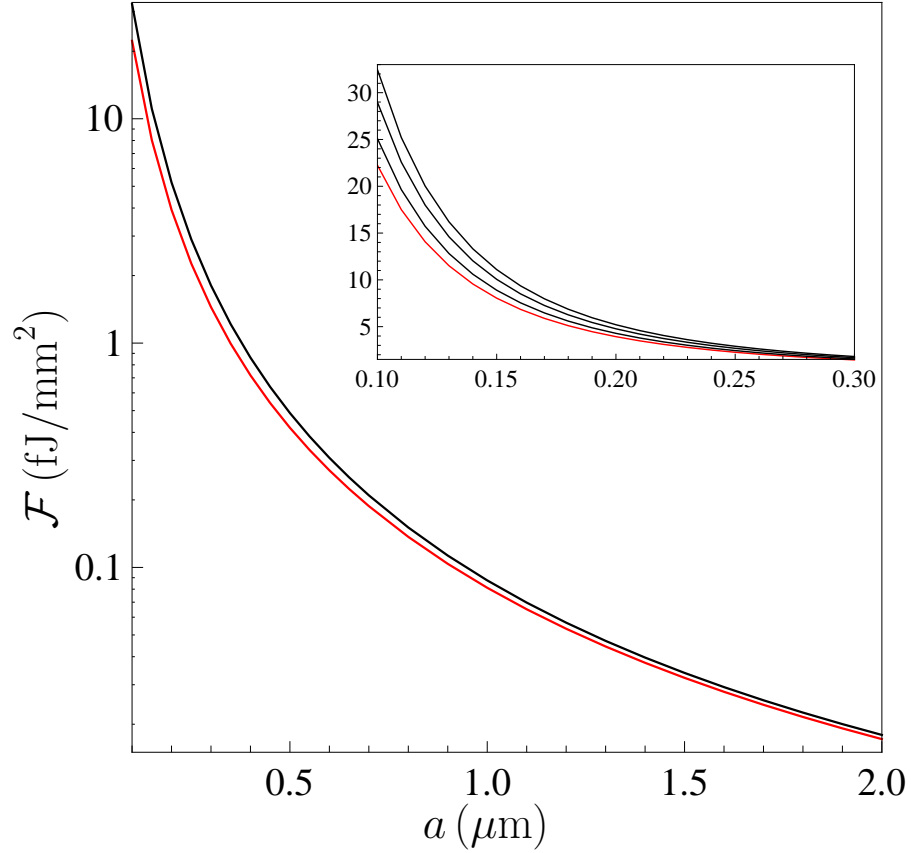


FIG. 6: The fluctuation-induced free energies of peptide films, deposited on Au substrate, which contain 0 and 0.4 volume fractions of water, are shown as the functions of film thickness by the bottom and top lines, respectively. In an inset, the free energy of peptide films containing 0, 0.1, 0.25, and 0.4 volume fractions of water are shown by the four lines plotted from bottom to top, respectively, using an uniform energy scale.

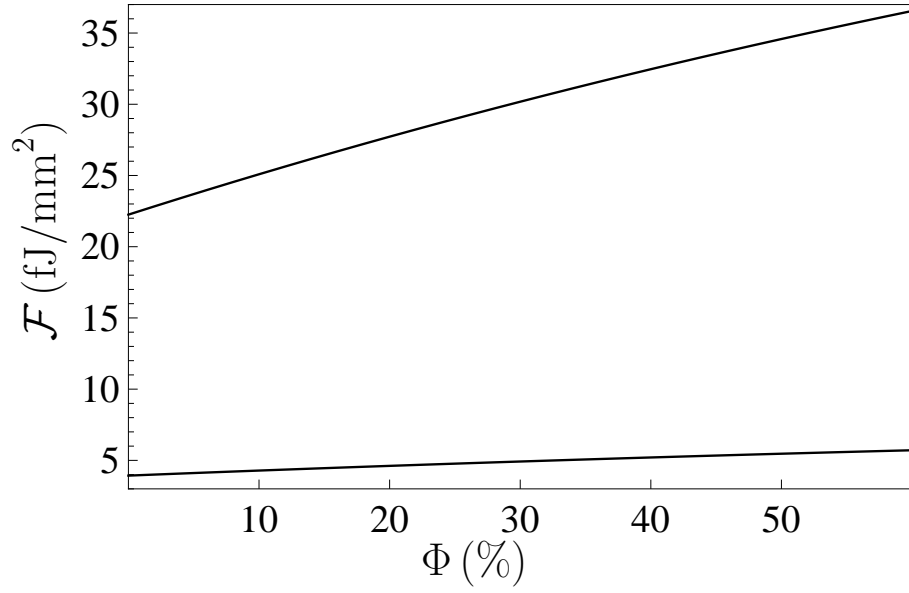


FIG. 7: The fluctuation-induced free energies of peptide films of thicknesses 200 and 100 nm deposited on Au substrate are shown as the functions of the fraction of water in the film by the bottom and top lines, respectively.

TABLE I: The values of the oscillator strengths C_j , oscillator frequencies ω_j and relaxation parameters g_j for the dielectric permittivity of distilled water.

j	C_j	ω_j (rad/s)	g_j (rad/s)
1	1.46	0.314×10^{14}	2.29×10^{13}
2	0.737	1.05×10^{14}	5.78×10^{13}
3	0.152	1.40×10^{14}	4.22×10^{13}
4	0.0136	3.06×10^{14}	3.81×10^{13}
5	0.0751	6.46×10^{14}	8.54×10^{13}
6	0.0484	1.25×10^{16}	0.957×10^{15}
7	0.0387	1.52×10^{16}	1.28×10^{15}
8	0.0923	1.73×10^{16}	3.11×10^{15}
9	0.344	2.07×10^{16}	5.92×10^{15}
10	0.360	2.70×10^{16}	11.1×10^{15}
11	0.0383	3.83×10^{16}	8.11×10^{15}